

Figure S1

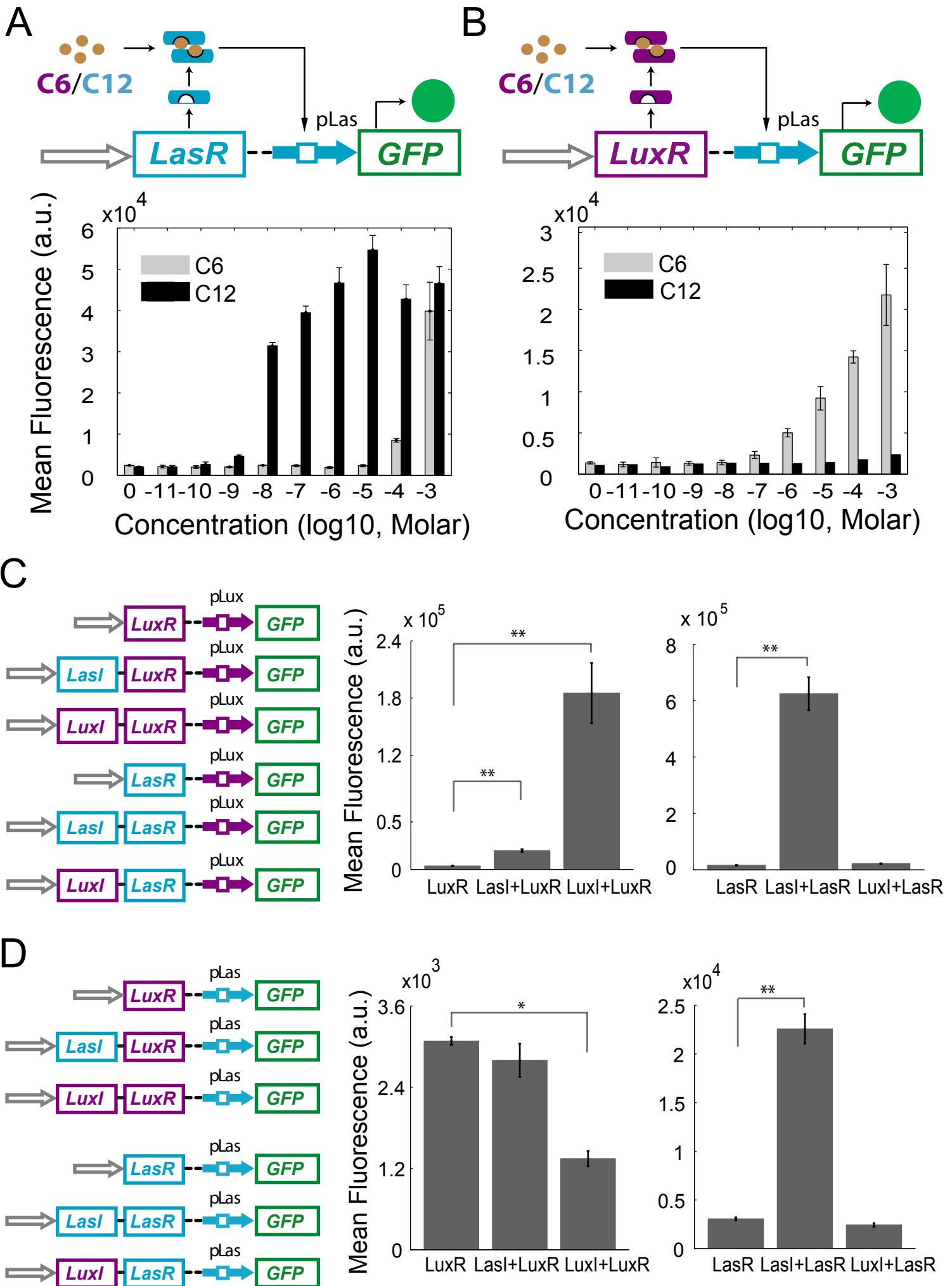
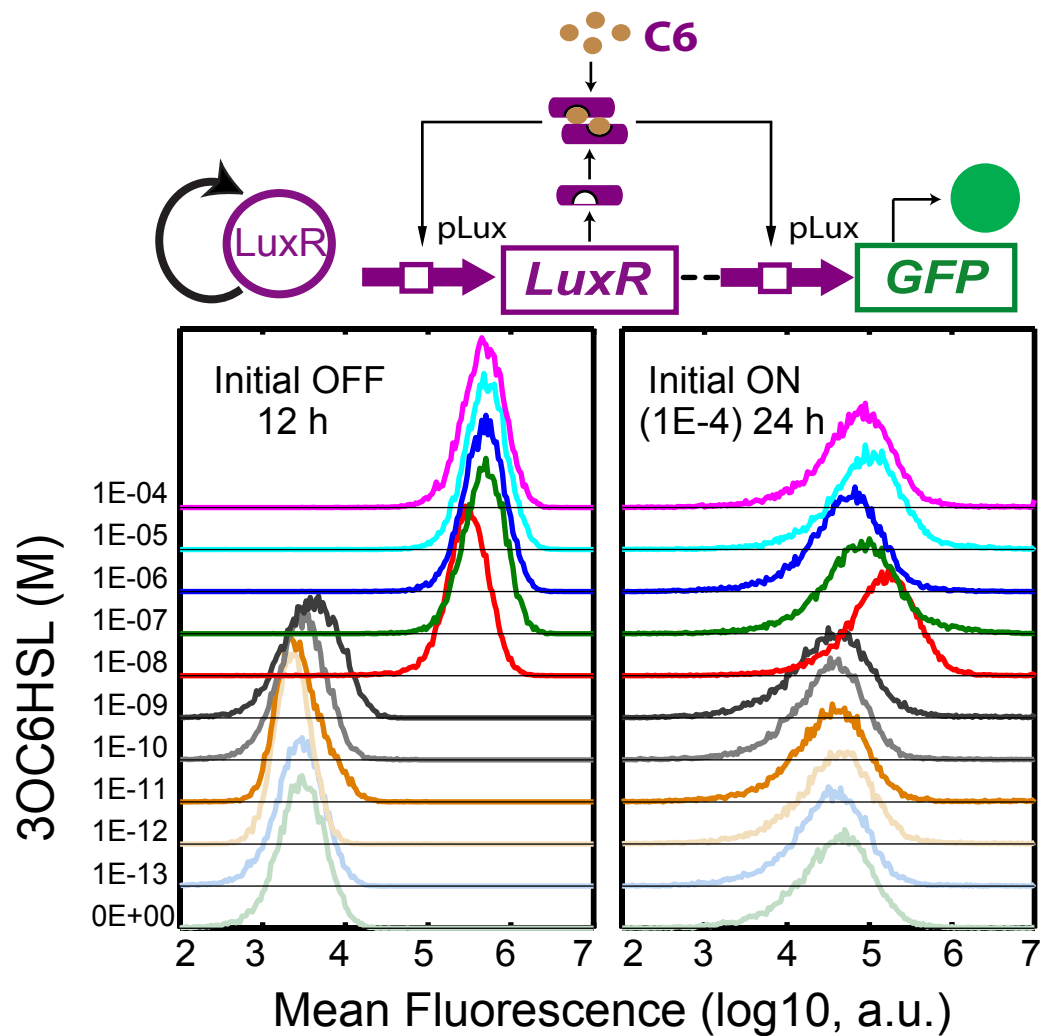


Figure S2

A



B

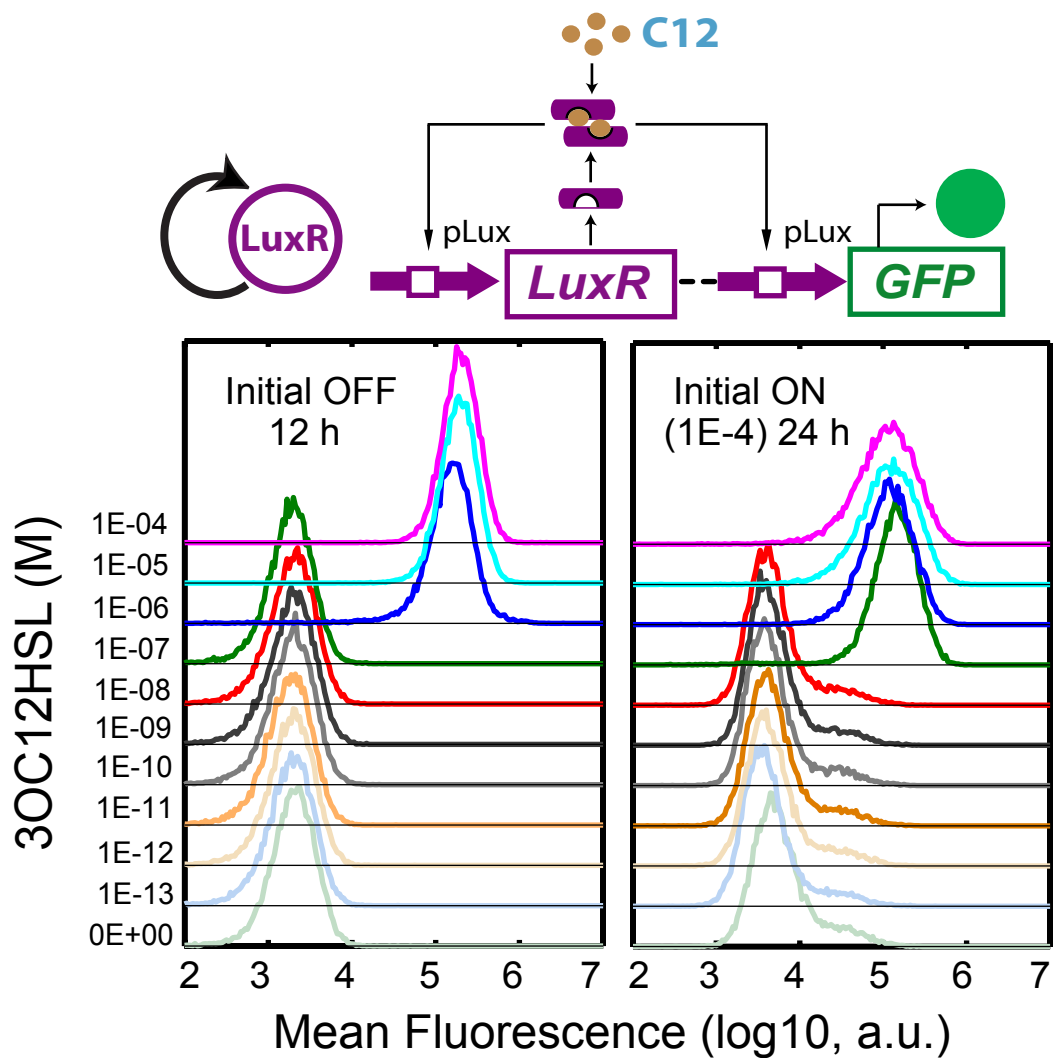


Figure S3

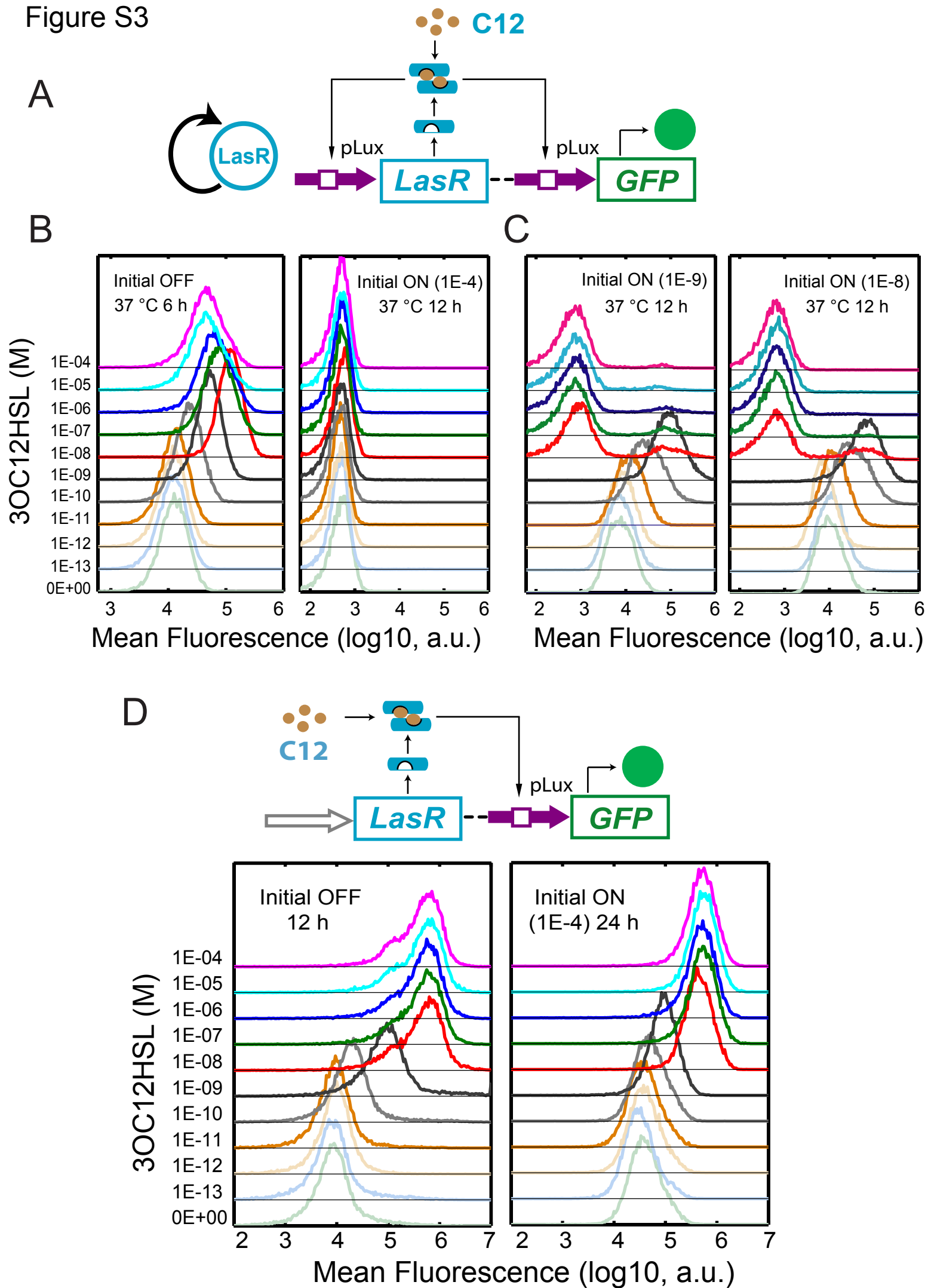
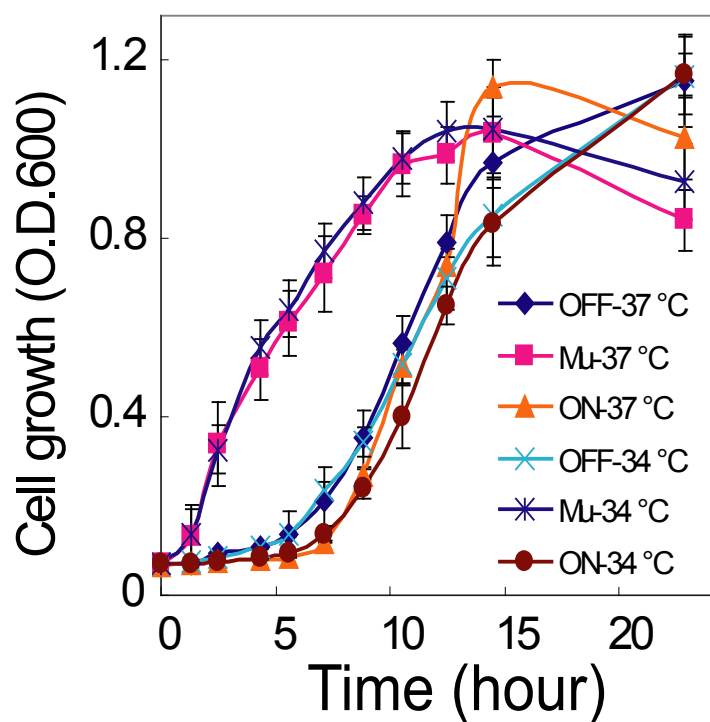
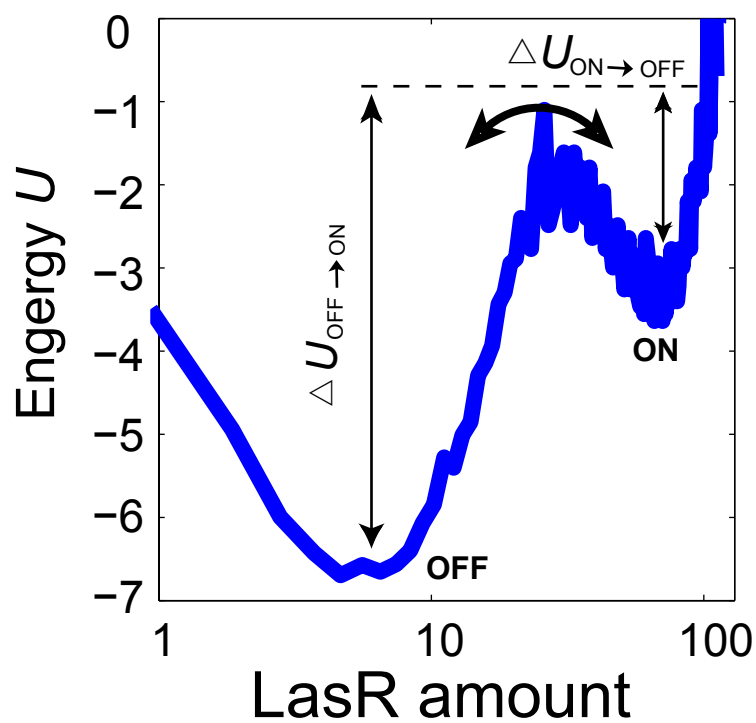


Figure S4

A



C



B

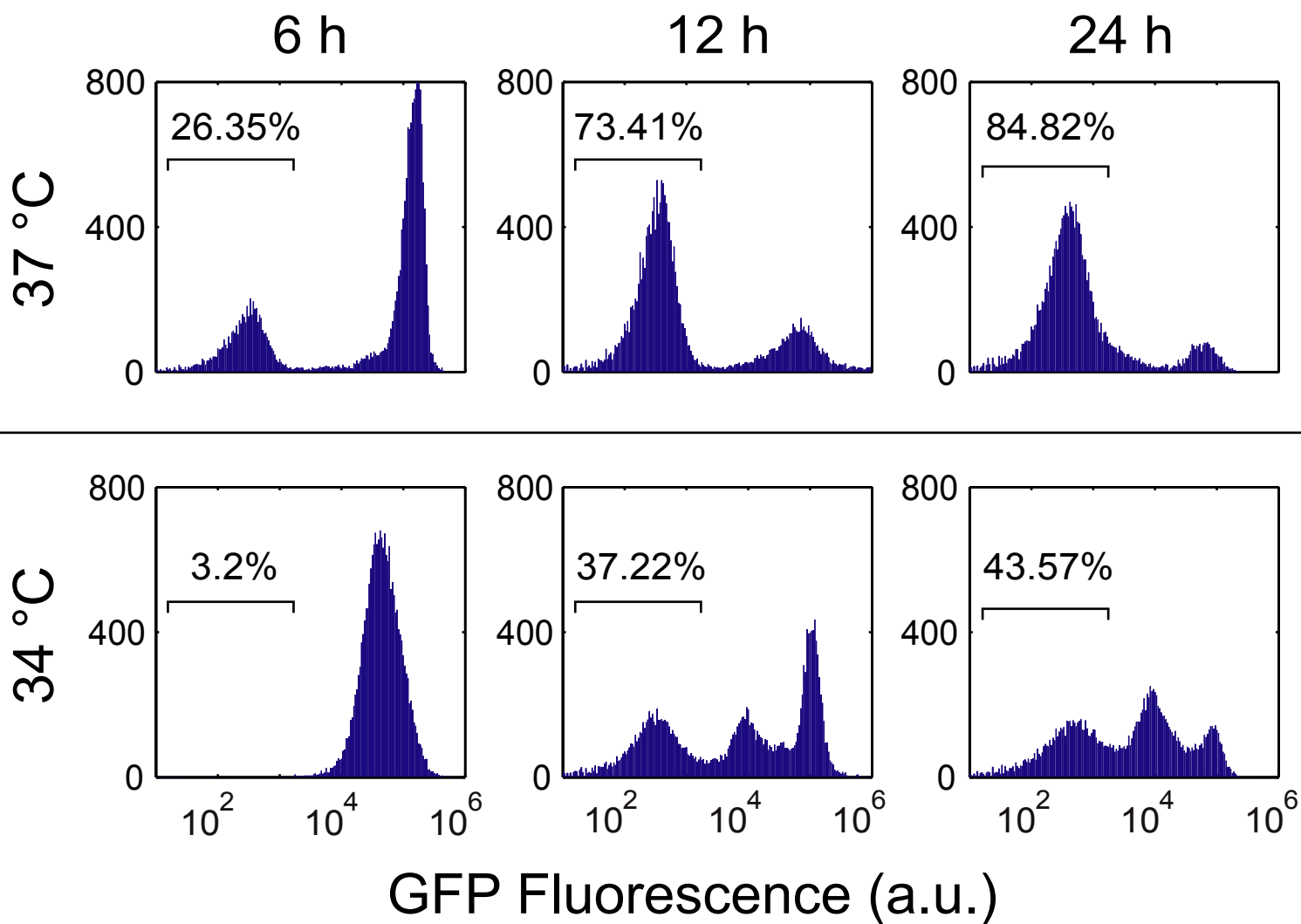
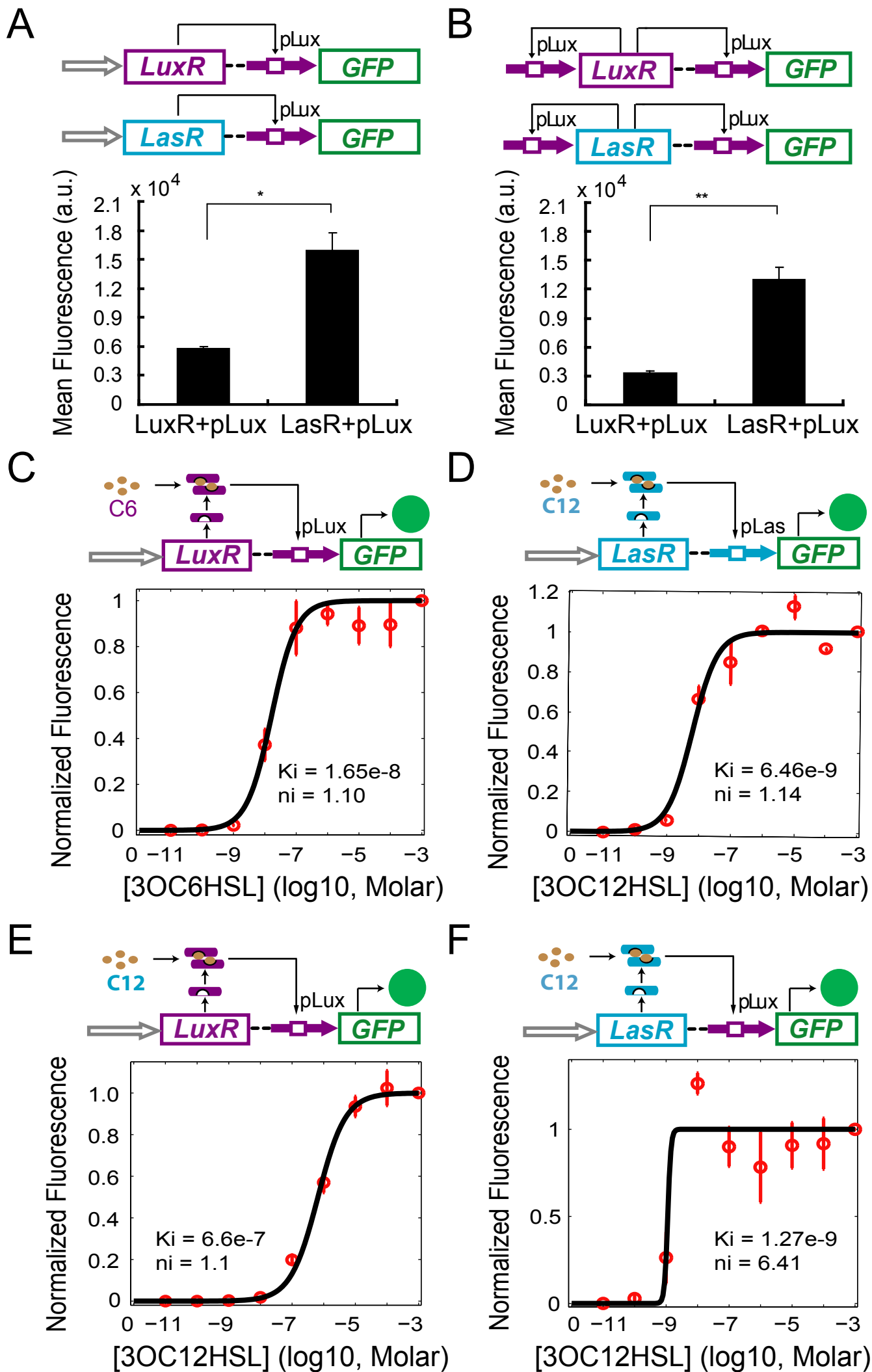


Figure S5



Supplemental Figure and Movie Legends:

Figure S1, related to Figure 1. QS crosstalk dissected using synthetic gene circuits. (A) High concentrations of C6 can crosstalk with LasR-pLas. Top panel: schematic diagram of the synthetic gene circuit (CP-LasR-pLas). Bottom panel: dose response of the circuit when induced with C6 or C12. Compared to original pair of LasR-C12, the pLas promoter can only be activated by LasR with extremely high C6 concentration (signal crosstalk). **(B)** Promoter crosstalk of C6-LuxR with pLas is observed under high concentrations of autoinducer. Top panel: schematic diagram of the circuit (CP-LuxR-pLas). Bottom panel: Dose response of this circuit when induced with C6 or C12. LuxR can bind with C6 to activate pLas starting from 10^{-6} M (promoter crosstalk), while it cannot with C12. **(C)** Characterizing the crosstalk with the pLux promoter using synthase genes. LuxR, with either LuxI or with LasI, can activate pLux, while LasR with LasI can activate pLux. Left: schematic diagram of the synthetic gene circuits constructed to test crosstalk. LasI (cyan) and LuxI (purple) synthesize C12 and C6 molecules in cells, respectively. Right: GFP fluorescence in cells carrying the circuits was measured by flow cytometry at 12 h. LasI with LuxR, and LasI with LasR can significantly activate pLux (signal crosstalk, and promoter crosstalk, respectively). **(D)** Characterizing the crosstalk to the pLas promoter using synthase genes. No significant crosstalk was observed for LuxR- or LasR-pLas combinations. Left: schematic diagram of the synthetic gene circuits constructed. Right: GFP fluorescence in cells carrying the circuits was measured at 12 h. Both LasI-LuxR and LuxI-LuxR cannot activate pLas, and the latter shows ~ two-fold inhibition, and no signal crosstalk is observed for LasR-pLas. All the data are averages of three independent measurements shown as mean \pm SD (* p <0.05, and ** p <0.01).

Figure S2, related to Figure 2. Hysteresis of the LuxR-pLux positive feedback circuit. (A) C6 induced hysteresis of the LuxR-pLux positive feedback circuit. Flow cytometry measurements of GFP expression for initial OFF cells (left) at 12 h and initial ON cells (right) at 24 h and 37 °C under different concentrations of C6 induction. Initial ON cells were collected from the cells induced with 10^{-4} M C6 for 6 hours and diluted twice into fresh media with the same concentrations of C6 at 12 h and 24 h. The positive feedback circuit displays

hysteresis with a bistable region from 0 to 10^{-8} M C6. No bimodal distribution was observed. **(B)** C12 induced hysteresis of the LuxR-pLux positive feedback circuit. Flow cytometry measurements of GFP expression for initial OFF cells (left) at 12 h and initial ON cells (right, induced with 10^{-4} M C12 for 6 hours before redilution) at 24 h and 37 °C under C12 induction. The initial ON cells were collected and diluted twice into new medium with the same concentrations of C12 at 12 h and 24 h. The positive feedback circuit displays hysteresis with a bistable region from 10^{-8} to 10^{-6} M C6. No bimodal distribution was observed.

Figure S3, related to Figure 3. Hysteresis of the LasR-pLux circuits. **(A)** Schematic representation of the LasR-pLux positive feedback loop induced with C12. **(B)** Flow cytometry measurements of GFP expression for initial OFF cells (left) at 6 h and initial ON cells (right) at 12 h and 37 °C under different concentrations of C12 induction. For initial OFF cells, GFP expression increases with C12 concentration, but begins to decrease uniformly when C12 induction exceeds 10^{-8} M. For initial ON cells (induced with 10^{-4} M C12 before redilution), all the samples exhibit unimodal minimal fluorescence signals that are even lower than the basal GFP expression of initial OFF cells. **(C)** Initial OFF cells were first induced with 10^{-9} or 10^{-8} M at 37 °C for 6 hours to become the new Initial ON cells, which were then collected and rediluted into fresh media with different doses of C12. These two Initial ON groups show a similar GFP expression pattern: unimodal distributions similar to the initial OFF cells for samples in the lower inducer concentrations of 0 to 10^{-9} M, and bimodal distributions within the higher concentration range of 10^{-8} to 10^{-4} M C12. GFP fluorescence was measured by flow cytometry at 12 h. **(D)** C12 induced hysteresis of the CP-LasR-pLux circuit. Flow cytometry measurements of GFP expression in initial OFF cells (left) at 12 h and initial ON cells (right, induced with 10^{-4} M C12 for 6 hours before redilution) at 24 h and 37 °C under C12 induction. Results show that the initial OFF and ON cells show a similar distribution pattern, and both exhibit unimodal expression without hysteresis.

Figure S4, related to Figure 4. **(A)** Growth curves for initial ON, OFF and Mutated cells in 10^{-8} M C12 at 37 °C and 34 °C. The initial ON and OFF cells' growth curves were similar, with a long lag phase in 10^{-8} M C12, while the Mutated cells directly entered exponential

growth phase. All populations reached stationary phase after about 15 hours. The three cell types show similar growth curves at 37 °C and 34 °C, indicating that growth temperature does not significantly influence their growth rate. **(B)** Temperature changes the transposition rate. Top: temporal evolution of the initial ON cells grown in 10^{-8} M C12 at 37 °C. Bottom: time course of the same initial ON cells grown in 10^{-8} M C12 but at 34 °C. Flow cytometry was used to measure the GFP fluorescence at 6 h, 12 h, and 24 h. For each measurement, the percentage of Mutated state cells was calculated. Data shows that higher temperature increases the transposition rate and IS10 transposase insertion, which promotes the transition from the ON state to the Mutated state. **(C)** Quasi-potential U and the transition dynamics between stable steady states in the LasR-pLux positive feedback system (without genetic mutation). The lower ‘valley’ (with lower potential U) is the stable OFF state and the higher is the stable ON state. According to the stochastic simulation, the energy barrier $\Delta U_{\text{OFF} \rightarrow \text{ON}}$ is much greater than $\Delta U_{\text{ON} \rightarrow \text{OFF}}$, which suggests it is easier for ON state cells to transition to the OFF state. The energy function is calculated according to the probability density distribution of steady state LasR concentrations in each cell.

Figure S5, related to Figures 2 and 4. Model parameter determination. **(A)** Comparison of the basal GFP expression from the pLux promoter between the two linear CP-LuxR-pLux and CP-LasR-pLux circuits. **(B)** Comparison of basal GFP expression from the pLux promoter between the two LuxR-pLux and LasR-pLux positive feedback circuits. All the data shows that the leakage from the pLux promoter in LasR-pLux circuits is greater than in LuxR-pLux circuits. All the data were averages of three independent measurements shown as mean \pm SD (* $p < 0.05$, and ** $p < 0.01$). Parameters determination from experimental tests: **(C)** the CP-LuxR-pLux circuit induced with C6; **(D)** the CP-LasR-pLas circuit induced with C12; **(E)** the CP-LuxR-pLux circuit induced with C12; **(F)** the CP-LasR-pLux circuit induced with C12. **(C)** and **(D)** are the original pairs used to test the functionality of all modules, while **(E)** and **(F)** were used to characterize the signal and promoter crosstalk. All of the red data points represent the mean of three independent measurements shown as mean \pm SD. The solid black curves, corresponding Hill coefficients (ni), and dissociation constants (K_i) between LuxR/LasR and C6/C12 were fitted from the dose response curves by the same fitting method

used in our previous work (Ellis et al., 2009; Wu et al., 2013).

Movie S1, related to Figure 5. A time lapse movie corresponding to Fig. 5A, for about 28 hours at 34 °C.

Table S1, related to Figure 1. Autoinducer information

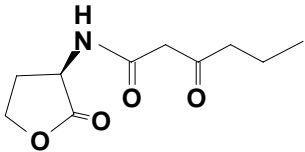
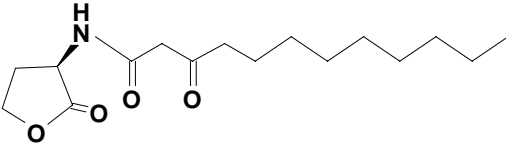
Full name	Molecular abbreviation	Molecular structure	Coding gene	Original binding regulator and promoter	Organism
N-(3-Oxohexanoyl)-L-homoserine lactone	3OC6HSL		LuxI (coding the enzyme, which synthesizes 3OC6HSL)	LuxR, pLux	<i>Aliivibrio fischeri</i>
N-(3-Oxododecanoyl)-L-homoserine lactone	3OC12HSL		LasI (coding the enzyme, which synthesizes 3OC12HSL)	LasR, pLas	<i>Pseudomonas aeruginosa</i>

Table S2, related to Figures 2 and 4. Parameters for the three positive feedback models

Parameters	Description	LuxR-pLux -3OC6HSL	LuxR-pLux -3OC12HSL	LasR-pLux -3OC12HSL	Source
k1	Transcription rate (min^{-1})	1.8	1.8	1.8	Ref.(Milo et al., 2010)
k2	Translation rate (min^{-1})	1.6	1.6	1.6	Ref.(Milo et al., 2010)
d1	LuxR/LasR degradation rate (min^{-1})	0.01	0.01	0.01	Ref.(Basu et al., 2005; Sayut and Sun, 2010)
d2	mRNA degradation rate (min^{-1})	0.33	0.33	0.33	Ref. (Bakshi et al., 2012; Milo et al., 2010)
c1	Leakage without LuxR or LasR protein (min^{-1})	0.08	0.08	0.08	Approximated according to Ref.(Danino et al., 2010)
c0	Leakage without AHL	0.007	0.007	0.03	Estimated and experiment indicated
Kd	Dissociation constant of LuxR-HSL dimerization	600	180	720	Estimated
Kn	Dissociation constant of [LuxR-HSL] ₂ binding DNA	2.6	14.7	177	Estimated
Ki	HSL concentration producing half occupation of pLux promoter	1.6e-8	6.6e-7	6.9e-9	Measured by experiments
ni	Hill coefficient	1.3	1.1	6.4	Measured by experiments

Table S3, related to Figure 4. Parameters for the genetic mutation event in the stochastic simulation of LasR-pLux positive feedback system

Parameters	Description	Value	Source
n	Cooperativity of IS10 transposase binding to the plasmid of LasR	5	Estimated and experiment indicated
K	Dissociation constant between transposase and the plasmid DNA	400	Estimated and experiment indicated
k3 (37 °C)	Transposition rate at 37 °C (min ⁻¹)	3.6e-6	Approximated according to experimental results and Ref.(Craig, 2002; Sousa et al., 2013)
k3 (34 °C)	Transposition rate at 34 °C (min ⁻¹)	4.0e-7	Approximated according to experimental results
c1	Transcription rate after gene mutation (min ⁻¹)	0.01	Estimated and experiment indicated
k1	Leakage without LasR protein after gene mutation (min ⁻¹)	0.005	Estimated and experiment indicated

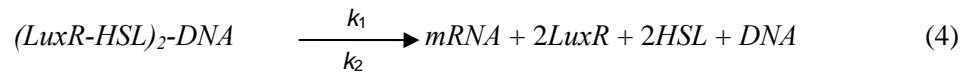
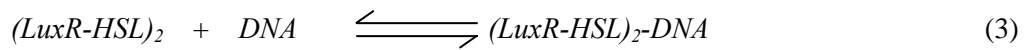
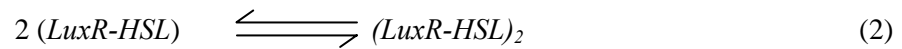
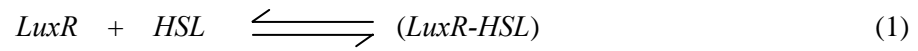
Table S4, related to Figure 1, 2, 3 and 4. Plasmids used in the circuits' construction. All materials are from the Registry of standard biological parts

Biobrick number	Abbreviation	Description
	in the paper	
BBa_R0062	pLux	Promoter activated by LuxR in concert with 3OC6HSL
BBa_R0079	pLas	Promoter activated by LasR in concert with 3OC12HSL
BBa_K176009	CP	Constitutive promoter family member J23107 actual sequence (pCon 0.36)
BBa_B0034	RBS	Ribosome binding site
BBa_B0015	T	Transcriptional terminator (double)
BBa_C0062	LuxR	LuxR repressor/activator
BBa_C0079	LasR	LasR activator
BBa_C0161	LuxI	Autoinducer synthetase for AI <i>from Aliivibrio fischeri</i>
BBa_C0178	LasI	Autoinducer synthetase for PAI from <i>Pseudomonas aeruginosa</i>
BBa_E0240	GFP	GFP generator
pSB1A3	pSB1A3	High copy BioBrick assembly plasmid

Supplemental Experimental Procedures:

Deterministic Model Construction

In the positive feedback loop circuit, LuxR production is controlled by the pLux promoter with only one LuxR-HSL binding site, which is bound and activated by the complex of LuxR and the autoinducer (3OC6HSL or 3OC12HSL, hereafter denoted as C6 and C12, respectively). GFP expression, as a reporter of the system, is regulated by the same pLux promoter and therefore follows the dynamics of LuxR. Therefore, we can directly analyze the LuxR dynamics in the model, comparing the output to the cells' fluorescence, without any loss of explanatory power. Since the LuxR-pLux and LasR-pLux positive feedback systems are characterized similarly and described by the same mathematical equations, we explain only the technical details for the LuxR-pLux positive feedback loop. Our model is based on the following biochemical reactions:



where *LuxR* is the monomer form of LuxR protein; *HSL* is the autoinducer 3OC6HSL; (*LuxR-HSL*) is the complex of LuxR bound with *HSL*; (*LuxR-HSL*)₂ is the dimer of (*LuxR-HSL*); (*LuxR-HSL*)₂-DNA represents (*LuxR-HSL*)₂ binding to the pLux promoter; *mRNA* is the messenger RNA of the LuxR gene; *k*₁ and *k*₂ are the transcription and translation rates, respectively; *d*₁ and *d*₂ are the degradation rates of mRNA and LuxR, respectively.

After C6 concentration reaches a certain threshold, LuxR binds to HSL molecules and forms the active LuxR monomers in the form of (*LuxR-HSL*) (Reaction 1). To quantitatively capture the relationship between the autoinducer concentration and the active LuxR

monomers, a Hill function is employed to represent the fraction of LuxR monomers bound by HSL (f):

$$f = [\text{HSL}]^{n_i} / ([\text{HSL}]^{n_i} + K_i^{n_i}) \quad [\text{Eq1}]$$

where n_i is the binding cooperativity (Hill coefficient) between LuxR and HSL, and K_i represents the dissociation constant between LuxR and HSL (the HSL concentration producing half conversion of LuxR monomers into *LuxR-HSL* complexes). It should be noted that different autoinducers will have different K_i values. Here we assume that the activator LuxR is abundant, and the fraction of active LuxR is independent from LuxR abundance in the cell.

LuxR needs to form a dimer to bind the promoter and activate transcription. We describe the relationship between the dimer and the monomer as the following expression:

$$[\text{LuxR}_2] = [\text{LuxR}]^2 / K_d \quad [\text{Eq2}]$$

where K_d is the dissociation constant for LuxR dimerization. According to reaction (2), two (*LuxR-HSL*) molecules bind together to form a dimer and activate transcription. Additionally, it is necessary to point out that even without autoinducer *LuxR*₂ can still bind the pLux promoter and initiate leaky transcription of downstream genes. Taken together, the concentration of the functional LuxR dimer that will bind to pLux and activate its transcription is:

$$C = (c_0 + f^2) * [\text{LuxR}]^2 / K_d \quad [\text{Eq3}]$$

Here C represents the concentration of functional LuxR dimer (*(LuxR-HSL)*₂ and *LuxR*₂); c_0 is the fraction of *LuxR*₂ that can recognize and bind pLux in the absence of autoinducers; K_d is the dissociation constant for dimerization.

*(LuxR-HSL)*₂ then recognizes and binds to the pLux promoter to form the *(LuxR-HSL)*₂-DNA complex together with RNA polymerase and other transcription factors to initiate transcription and produce mRNA (Reactions 3 and 4). So the expression of mRNA can be modeled as:

$$S_m = c_l + k_l C / (C + K_h) \quad [\text{Eq4}]$$

where S_m represents the production of mRNA; c_l represents the basal mRNA expression

without LuxR protein; k_l is the transcription rate; K_n is the dissociation constant between C and pLux promoter.

After transcription, mRNA is translated into LuxR protein (Reaction 5). Here we simplify the whole translation process and capture the production of LuxR protein in the form of:

$$S_p = k_2 * [\text{mRNA}] \quad [\text{Eq5}]$$

where S_p represents the synthesis of LuxR and k_2 is the translation rate.

Next, we take the constitutive degradation of mRNA in the cell into account (Reaction 6) with the equation:

$$D_m = d_1 * [\text{mRNA}] \quad [\text{Eq6}]$$

where d_1 is the degradation rate of mRNA.

Similarly, the degradation of LuxR protein (Reaction 7) is:

$$D_p = d_2 * [\text{LuxR}] \quad [\text{Eq7}]$$

where d_2 is the degradation rate of LuxR.

Finally, we combine the synthesis and degradation (Eq4, 5, 6, and 7) to find the rates of change of the concentrations of mRNA and LuxR:

$$\begin{cases} d[M]/dt = S_m - D_m \\ d[R]/dt = S_p - D_p \end{cases} \quad [\text{Eq8}]$$

where M and R represents mRNA of LuxR and LuxR monomers, respectively. Combining all the parameters, the two ODE equations can be rewritten as follows:

$$\begin{cases} \frac{d[M]}{dt} = c_1 + \frac{k_1 C}{C + K_n} - d_1 [M]; \\ \frac{d[R]}{dt} = k_2 [M] - d_2 [R]. \end{cases} \quad \text{Where} \quad \begin{cases} C = \frac{(c_0 + f^2) \cdot [R]^2}{K_d} \\ f = \frac{[\text{HSL}]^{n_i}}{[\text{HSL}]^{n_i} + K_i^{n_i}} \end{cases} \quad [\text{Eq9}]$$

These two ordinary differential equations were used to model the three positive feedback loops: LuxR-pLux-C6, LuxR-pLux-C12, and LasR-pLux-C12. Owing to the signal and promoter crosstalk, the dissociation constants K_i , K_d , and K_n may be different, as may also be the case with the Hill coefficients and leaky expression without autoinducer. Setting of parameter values is introduced below.

Stochastic Simulation Coupled with Genetic Mutation

The Gillespie algorithm was employed to perform stochastic simulations of the positive feedback loops (Gillespie, 1977). According to our deterministic model (Eq9), two equations capture the time evolution of the biochemical reactions. In this model, there are four independent events in total – mRNA production, mRNA decay, LuxR production, and LuxR decay – which are translated directly to the stochastic model. Simulation data was collected for 8000 cells, and each simulation was run for 40000 steps.

The energy-like function $U(x)$, which denotes the probability and direction of transitions between attractors in a noisy environment, can also be used to interpret state transitions (Zhou et al., 2012). After finishing all simulations, we first calculated the amount of LasR present in each cell (assuming the cells had reached steady state), then divided by the total number of cells. This yielded a probability density distribution of steady state LasR concentrations, which was used to calculate the energy function $U(LasR)$ by the following approach (Zhou et al., 2012):

$$U(LasR, t) \sim -\ln(P(LasR), t) \quad [\text{Eq10}]$$

where $P(LasR, t)$ is the steady-state probability for each LasR concentration at a given time t . In practice, the $P(LasR, t)$ was derived from the following equation:

$$P(LasR) = \text{hist}(LasR) / \text{Cellnum} \quad [\text{Eq11}]$$

where $\text{hist}(LasR)$ is a histogram of the amount of LasR in each cell and Cellnum is the total number of simulated cells. The energy-like function U gave us a more vivid and direct understanding of the quasi-potential landscape and the transition dynamics between stable steady states in this positive feedback system. The transition rates between ON and OFF states are decided by the energy barrier ΔU (Figure S4C). Unlike the typical bimodality emerged from bistable systems, C12-LasR-pLux positive feedback loop displayed an asymmetric bimodal distribution at a population level, which only happened from ON state to OFF state. The model suggests that this asymmetry comes from the different energy barrier of switching between ON and OFF states (Figure S4C).

To take the genetic mutation in the LasR-pLux positive feedback circuit into account, we

added another event in addition to mRNA and LasR production and degradation. Since the genetic mutation only happened in initial ON cells, and because it is easier for cells in high C12 concentration to mutate, we inferred that more LasR in the cell resulted in a higher mutation probability. Moreover, the mutation occurred in the LasR open reading frame, so theoretically the mutation probability is positive as long as the LasR gene is present. Here, we used a Hill function to describe the probability of mutation:

$$Pm = [LasR]^n / (K^n + [LasR]^n) \quad [Eq11]$$

where Pm represents the probability of mutation; n is the Hill coefficient indicating the cooperativity of mutation causing factors related to LasR concentration; and K represents the dissociation constant in the complicated biochemical reactions. In the Gillespie simulation, the mutation event, independent of the other four events, was described mathematically as:

$$Mu = k_3 * Pm * [LasR] \quad [Eq12]$$

where k_3 is the transposition rate; $[LasR]$ is the amount of LasR in the cell at a given time, and Pm is the probability of mutation as described above. Generally, once the mutation has happened, the LasR gene is broken into two parts and the functional mRNA of LasR cannot be produced any more. Mutated cells theoretically retain the ability to switch state. However, the probability of this occurring is small. In practice, for each cell, when the mutation event had occurred, the transcription rate (k_l) and leaky expression from pLux (c_l) were reduced to very low values, the cell would remain mutated, and the simulation was ended. By tuning the transposition rate, we fit the parameters according to experimental data, which we then used to make predictions.

Next, since the ON, OFF, and Mutation cells have different growth curves under the same experimental conditions, growth rate differences between the three populations were added into the model. From the growth curves, it can be seen that the initial ON and OFF cells' growth curves were similar, with a long lag phase in 1e-8 M C12, while the Mutation cells directly entered exponential growth. All three populations went to stationary phase after about 15 hours (Figure S4A). Instead of using a population balance model, we employed a simple and efficient method to combine the stochastic model with population dynamics. The cells

with greater growth rate would acquire an extra advantage in their final quantity: each of the three original populations was multiplied by its relative growth rate and then its ratio in the three populations was adjusted.

To simplify the case, we chose three time points (2.5 h, 7.1 h and 12.5 h) and compared their O.D. values (by $OD^{\text{Mutation}}/OD^{\text{ON}}$, $OD^{\text{OFF}}/OD^{\text{ON}}$, and $OD^{\text{ON}}/OD^{\text{ON}}$: ON cells grew slowest) and then made an average to get an averaged relative growth rate, which then was taken into the simulation results. So the final amount of Mutation cells (Fmu), OFF cells ($Foff$) and ON cells (Fon) are:

$$Fmu = Smu * (OD^{\text{Mutation}}/OD^{\text{ON}});$$

$$Foff = Soff * (OD^{\text{OFF}}/OD^{\text{ON}});$$

$$Fon = Son * 1;$$

where Smu , $Soff$, and Son are the primary number of cells which finished the simulation in the Mutation, OFF, and ON states, respectively. Therefore, the proportions of Mutation cells (Pmu), OFF cells ($Poff$), and ON cells (Pon) are:

$$Pmu = Fmu/(Fmu + Foff + Fon);$$

$$Poff = Foff/(Fmu + Foff + Fon);$$

$$Pon = Fon/(Fmu + Foff + Fon);$$

In this way, the population with a greater growth rate acquired an advantage in its quantity under identical conditions.

Determinations of parameter values

In the *E.coli* cells, even though the transformed plasmid is high-copy, there is also a maximum expression value. According to the B10NUMB3R5 database(Milo et al., 2010), each protein generally has no more than 1000 copies. Therefore, we chose 1000 molecules per cell to be the maximum expression value of LuxR and LasR. All other parameters were adjusted under this assumption.

Specifically, the transcription rate (k_1), translation rate (k_2), and degradation rates of mRNA and LuxR (d_1 and d_2 , respectively) were estimated from previous reports and the B10NUMB3R5 database (Table S2). Since pLux was the only promoter used in the positive feedback circuits, the leaky expression without LuxR or LasR (c_1) did not change between

simulations, and it was estimated to be 0.08 min^{-1} . In addition, according to experimental results, basal GFP expression in the absence of autoinducers (c_0) in the LasR-pLux positive feedback circuit is about three times larger than in its LuxR-pLux counterpart (Figure S5A and S5B). Therefore c_0 was set to 0.03 and 0.007 for LasR-pLux and LuxR-pLux, respectively. The Hill coefficients (n_i) and dissociation constants (K_i) between LuxR/LasR and the C6/C12 were fitted from the dose response curves (Figure S5C-S5F) by the same fitting method used in our previous work (Ellis et al., 2009; Wu et al., 2013). Considering experimental variations, parameters were adjusted within 10% relative error.

The generic parameters K_d and K_n are constant and fit to make the model consistent with with experimental results (Figure 2B and 2C). With these fitted parameters, our model captured the experimental hysteresis results and provided insights to understand the difference between the three positive feedback loop variants induced by QS crosstalk. For example, K_d in LuxR-pLux-C12 positive feedback was smaller than in LuxR-pLux-C6, while K_n was larger for LuxR-pLux-C12. This suggests that C12 might bind more easily to LuxR (relative to C6), but the original LuxR-C6 pair has higher affinity for the pLux promoter. Additionally, K_n in the LasR-pLux positive feedback loop is much bigger for LasR-C12 than for either LuxR-C6 or LuxR-C12, which indicates that the LasR-C12 dimer has less affinity for pLux, and therefore it is more difficult for the system to reach saturation. The parameter combination for the LasR-pLux positive feedback loop was used in the stochastic simulation and for predicting trimodality.

To fit the probability of the LasR gene's mutation against experimental results at 37°C , we first approximated the Hill coefficient (n) and the dissociation constant (K) based on the difference between fluorescence values at the ON and OFF states. Different n and K combinations were generated, and it was discovered that $n = 5$ and $K = 400$ best fit the experimental data (Figure 4A and 4B). In addition, previous reports indicated that transposition rates of IS elements in *E.coli* usually range from $1\text{e-}3$ to $1\text{e-}7 \text{ min}^{-1}$ (Craig, 2002; Sousa et al., 2013). So the transposition rate in our model was estimated ($k_3 = 3.6\text{e-}6 \text{ min}^{-1}$) according to the final experimental data (Figure 4B). To predict the trimodal response, k_3 was adjusted but all the other parameters were held constant. With $k_3 = 4.0\text{e-}7 \text{ min}^{-1}$, the

simulation exhibited trimodality, which was validated by the experimental results at 34 °C (Figure 4D and 4E).

All the parameter values are listed in Table S2 and S3.

Mutation verification by DNA sequencing

For the initial ON cells growing in 10^{-10} to 10^{-4} M C12, plasmids were extracted, digested for genotyping, and sequenced. Several primers were used to check for mutation. Following the order of assembly shown in Supplementary Fig. 16b, these primers were: BB-N-Forward, LasR-C-Forward, GFP-N-Reverse, BB-C-Reverse, and GFP-C-Forward. Descriptions and sequencing results for each primer are below. Combining these results, we concluded that the mutation happened within the LasR gene, and the other fragments and backbone were correct.

For convenience, all fragments are highlighted: pLux promoter: yellow; ribosomal binding site: blue; LasR: cyan; IS10 transposase: pink; Terminator: red; GFP generator: green; pSB1A3 vector: grey.

BB-N-Forward

Sequence: TGCCACCTGACGTCTAAGAA

Description: Forward, starting from the N terminal of the multiple cloning site (MCS)

Sequencing with BB-N-Forward on the vector verified the promoter pLux (yellow), the ribosomal binding site (blue), part of LasR (cyan, 681 bp), and a new inserted sequence (pink). This new sequence was determined to be part of an IS10 transposase gene according to BLASTn results from NCBI. The transposon target site is also marked (Bold black, highlighted pink). Sequencing results are as follows:

>LasR-pLux-PF-BBF 1360 ABI

1→

```
CACGGAACTTAACCTATACAAATAGGCGTATCACGAGGCAGAATTTTCAGA
TAAAAAAAAATCCTTAGCTTTTCGCTAAGGATGATTTCTGGAATTCGCGGCC
GCTTCTAGAGACCTGTAGGATCGTACAGGTTTACGCAAGAAAATGGTTTG
TTATAGTCGAATAAA TACTAGAGAAAGAGGAGAAA TACTAGATGGCCTTG
GTTGACGGTTTTCTTGAGCTGGAACGCTCAAGTGGAAAATTGGAGTGGAG
CGCCATCCTCCAGAAGATGGCGAGCGACCTTGGATTCTCGAAGATCCTGT
TCGGCCTGTTGCCTAAGGACAGCCAGGACTACGAGAACGCCCTTCATCGTC
GGCAACTACCCGGCCGCTGGCGGAGCATTACGACCGGGCTGGCTACGC
GCGGGTCGACCCGACGGTCAGTCACTGTACCCAGAGCGTACTGCCGATTT
TCTGGGAACCGTCCATCTACCAGACGCGAAAGCAGCACGAGTTCTTCGAG
GAAGCCTCGGCCCGCCGCTGGTGTATGGGCTGACCATGCCGCTGCATGG
TGCTCGCGGCGAACTCGGCGCGCTGAGCCTCAGCGTGGAAGCGGAAAACC
```

GGGCCGAGGCCAACCGTTTCATAGAGTCGGTCCTGCCGACCCTGTGGATG
 CTCAAGGACTACGCACTGCAAAGCGGTGCCGACTGGCCTTCGAACATCC
 GGTGAGCAAACCGGTGGTTCTGACCAGCCGGGAGAAGGAAGTGTTCAGT
 GGTGCGCCATCGGCAAGACCAGTTGGGAGATATCGGTTATCNTGCACTGC
 TCGGAAGCCAATGTGAACTTCCATATGGGAAATATTCGGCGGAAGTTCGG
 TGTGACCTCCCGC**CGCGTAGCG**CTGAGAGATCCCCTCATAATCCCCCAA
 GCGTAACCATGTGTGAATAAATTTTGAGCTAATAGGGTTCAGCCACGAG
 TAAGTCTTCCCTTTGTATTGTGTAACCAGAATGCCGCAAACTTCCATGC
 CTAAGCGAACTGTTGAAAGTACGTTTCGATTTCTGACTGTGTTAACCTGA
 AAGTGCTTGGTCCCACCTTGTTCCTGAACATGAACGCCCCGCAAGCCAAC
 ATGTTAGTTTGAAACTTCAGGGGAATTACCAACAGGAAATCATAAACGC
 TCTGAACCTTGCTCGTTTGGGTTTGGGGGAAGGGCCTAATTTCCGGAGGG
 CAGGAACTTTTTTCAGGTTTCGGGAAAGGGGGTTTTTTTTCAATTCTTTC
 ATTTTTCCCTTCTTCAAAAAAAAAAATATTATAAAAAAAAAAAGTTTTGGTG
 TGGGGGGGGGGTTTTGTTTAAATATTTTTTCTAACCAACGCGGGGAAAGA
 AAATATTTTT

Note:

- Highlight (yellow, 111-165): R0062, pLux promoter;
- Highlight (blue, 174-185): B0034, Ribosome binding site;
- Highlight (cyan, 192-872): C0079, LasR (part);
- Highlight (pink, 873-1211): IS10 transposase (part);
- CGCGTAGCG**: target site for transposition.

LasR-C-Forward

Sequence: TGGGTCTTATTACTCTCTAA

Description: Forward, starting from the C terminal of LasR

Sequencing with LasR-C-Forward showed that the sequence remained as expected – terminator (red), pLux promoter (yellow), and GFP generator (green) from left to right – which shows the absence of mutation. Sequencing results are as follows:

> LasR-pLux-PF-LasRC-F 1345 ABI

1→

CGGGGGCTCAAATAAAACGAAAGGCTCAGTCGAAAGACTGGGCCTTTCGT
 TTTATCTGTTGTTTGTTCGGTGAACGCTCTCTACTAGAGTCACACTGGCTC
 ACCTTCGGGTGGGCCTTCTGCGTTTATA**TACTAGAG**ACCTGTAGGATCG
 TACAGGTTTACGCAAGAAAATGGTTTGTATAGTCGAATAAA**ACTAGAG**
 TCACACAGGAAAGTACTAGATGCGTAAAGGAGAAGAACTTTT**ACTGAG**
 TTGTCCCAATTCTTGTGAATTAGATGGTGATGTTAATGGGCACAAATTT
 TCTGTCAGTGGAGAGGGTGAAGGTGATGCAACATACGGAAA**ACTTACCCT**
 TAAATTTATTTGCACTACTGGAAA**ACTACCTGTTCCATGGCCAACACTTG**
 TCACTACTTTTCGGTTATGGTGTTCAATGCTTTGCGAGATACCCAGATCAT

ATGAAACAGCATGACTTTTTCAAGAGTGCCATGCCCGAAGGTTATGTACA
 GGAAAGAACTATATTTTTCAAAGATGACGGGAACTACAAGACACGTGCTG
 AAGTCAAGTTTGAAGGTGATACCCTTGTTAATAGAATCGAGTTAAAAGGT
 ATTGATTTTAAAGAAGATGGAAACATCTTGGACACAAATGGAATACAA
 CTATAACTCACACAATGTATACATCATGGCAGACAAACAAAAGAATGGAA
 TCAAAGTAACTTCAAAATTAGACACAACATGAAGATGGAAGCGTTCAA
 CTAGCAGACCATTATCAACAAAATACTCCAATTGGCGATGGCCCTGTCCT
 TTTACCAGACAACCATTACCTGTCCACACAATCTGCCCTTTCGAAAGATC
 CCAACGAANAGAGAGACCACATGGTCCTTCTTGAGTTTGTAACAGCTGCT
 GGGATTACACATGGCATGGATGAACTATACAAATAATAACTAGAGCCA
 GGCATCAAATAAAACGAAAGGCTCAGTCGAAAGACTGGGCCTTTCGTTTT
 ATCTGTTGTTTGTGCGGTGAACGCTCTCTACTAGAGTCACACTGGCTCACC
TTCGGGTGGGCCTTTTCTGCGTTTATATACTATTAGCGGGCGCTGCAGGC
 TTCCTCGCTCACTGACTCCCCTGCGCCTCGGTGTTTCGGGCTGGCGGGA
 AGCGGGTATCAGCTTCACTCCAAGGGGGGTAATACGGTTTTTCCCCC
 AAAATCCGGGGGATAAACACCCGGGAAAAAAAAAACTTGGTGAAACC
 AAAAAGGGGCCCCACAAAAAGGGGCCCGGGAAAACCCGGTAAAAAAA
 AAGGGGCCCCCGGCGGTGTTGTTCTGGTGGTGGGGGTTTTTTTT

Note:

- Highlight (red, 8-129): B0015, Terminator;
- Highlight (yellow, 138-192): R0062, pLux promoter;
- Highlight (green, 193-1077): E0240, GFP generator;

GFP-N-Reverse

Sequence: GTGCCCATTAACATCACCATC

Description: Reverse, starting at 55th bp from the N terminal of GFP

Sequencing with GFP-N-Reverse showed that the sequence was not the same as expected. From left to right, these results showed: part of GFP (green), pLux promoter (yellow), terminator (red), C terminal of LasR (cyan), and a new inserted sequence (pink). This new sequence was demonstrated to be part of an IS10 transposase gene according to BLASTn results from NCBI. The transposon target site is also marked (Bold black, highlighted pink). Sequencing results are as follows:

>LasR-pLux-PF-GFPN-R 1403 ABI

1→

GGGGGGGGGTTG**GAAAAGTTGCTTCTCCTTTACGCATCTAGTACTTTCC**
TGTGTGACTCTAGTATTTATTCCCTTTTAGCAAACCATTTTCTTGCGTAA
 ACCTGTACGATCCTACAGGTCTCTAGTA**TATAAACGCAGAAAGGCCACC**
 CGAAGGTGAGCCAGTGTGACTCTAGTAGAGAGCGTTCACCGACAAACAAC
 AGATAAAACGAAAGGCCAGTCTTTCGACTGAGCCTTTCGTTTTATTGA
TGCCTGGCTCTAGTATTATTAGAGAGTAATAAGACCCAAATTAACGGCCA

TAATGGC**CGCTACGCG**CTGATGAATCCCCTCATGATTTTCGGCAAAAATCA
TTAATGTGAGGTGGATACTTGTCTTGCCAGATGATCAAATGGTTTCGCGT
AAACTCTTGAATCAGACCACATGATGTGCGATCTCGATATTTTACATCAC
TCTCTTTAAGAATTCTGCCCTGAATTACAGTTAGAACGACTCAACAGCTG
AACGTTGCGCTTGTACGCGCTTACTTGAGTGTAACACTCTCACTCTTACC
GAAATGGTTCGTAACCTGACAACCTAAGTGAGATCAAAACATAACATCAA
ACGACTCGACGGATTGGTATGTAATCGTCACCTCCGCAAAGAGCGACTCG
CTGTATACCGTTGGCCTGCTATCTATATCTGTTTCGGGCAATACGATGCC
ATTGTAGTTGGTGACTGGTCTGATATTCGAGAGCCTAAACAACCTTATCGT
GGTTGCGAGCTTCAGTCGCACTACCTGGTCGTTCTGATACTCTTTATGAG
AAAGCGTCCCATCTTCCGATCTTATGCTCAAGAAAGCTCATGATCATT
TCTAGCCGATCTTGTGATAGGTCATCGGAGAACTCCACTCTCGCTCATT
GTCAGGGATGTGGGCTTTTAAGGGACGTGGTATAATCCCTTGGAAAATTT
GGGTAGGTACTGGGTTACTCGAAGAGGAAGGAAAATTTTCATATGCGGGAC
CTTAGGAAGGGAAAACCGGGAAACCATTACAGCACTTA**ACTGTTTTTTGT**
TCTCTATACCCCTCCAAAATTTTGGTGTTTAAAAGTGTTTAATTAAAAAA
AATTCCAATTTCTAGTGCAAATGTCGTTTTTAAAAAATTTCTTTTGTCTAA
GGGCTGAAGAAATTTGACCTTTCTGCAGGGGAAACCTTTTGTCTCACCG
CCCAGCAATTTAAAAACTTTCTTTCTGCACGGGTGGGGCAGGGGGAGACCC
GGGAGGTCCCTTTTTTCCACCTAACTTTTTTCGCCTGTTGTTAAAAAATTAC
AAAACACACCCCTACCAAATCTCTTTTTTATAAAATTTACCTCCTTCTTA
GGAATAGCCCGAGAGTAGGCCAAAAAATATATTAAAAAAATTAACAC
TCT

Note:

- Highlight (green, 14-57): E0240, GFP generator (N terminal);
- Highlight (yellow, 66-120): R0062, pLux promoter;
- Highlight (red, 129-257): B0015, Terminator;
- Highlight (cyan, 266-307): C0079, LasR (C terminal);
- CGCTACGCG**: target site for transposition (duplication).
- Highlight (pink, 317-1038): IS10 transposase (part);

BB-C-Reverse

Sequence: AATACCGCCTTTGAGTGAGC

Description: Reverse, starting from the C terminal of MCS on the plasmid

Sequencing with BB-C-Reverse verified the GFP generator (green) and pLux promoter (yellow), which indicate a lack of mutation. Sequencing results are as follows:

> LasR-pLux-PF-BBR 1382 ABI

1→

GGGCGCCATCGTACGACCGAGCGCAGCGAGTCAGTGAGCGAGGAAGCCTG

CAGCGGCCGCTACTAGTATATAAACGCAGAAAGGCCACCCGAAGGTGAG
CCAGTGTGACTCTAGTAGAGAGCGTTCACCGACAAACAACAGATAAAACG
AAAGGCCAGTCTTTTCGACTGAGCCTTTTCGTTTTATTTGATGCCTGGCTC
TAGTATTATTATTTGTATAGTTCATCCATGCCATGTGTAATCCCAGCAGC
TGTTACAAACTCAAGAAGGACCATGTGGTCTCTCTTTTCGTTGGGATCTT
TCGAAAGGGCAGATTGTGTGGACAGGTAATGGTTGTCTGGTAAAAGGACA
GGGCCATCGCCAATTGGAGTATTTTGTGATAATGGTCTGCTAGTTGAAC
GCTTCCATCTTCAATGTTGTGTCTAATTTTGAAGTTAACTTTGATTCCAT
TCTTTTGTGTCTGCCATGATGTATACATTGTGTGAGTTATAGTTGTAT
TCCAATTTGTGTCCAAGAATGTTTCCATCTTCTTTAAAATCAATACCTTT
TAACTCGATTCTATTAACAAGGGTATCACCTTCAAACCTTGACTTCAGCAC
GTGTCTTGTAGTTCCCGTCATCTTTGAAAAATATAGTTCTTTCCTGTACA
TAACCTTCGGGCATGGCACTCTTGAAAAAGTCATGCTGTTTCATATGATC
TGGGTATCTCGCAAAGCATTGAACACCATAACCGAAAGTAGTGACAAGTG
TTGGCCATGGAACAGGTAGTTTTCCAGTAGTGCAAATAAATTTAAGGGTA
AGTTTTCCGTATGTTGCATCACCTTCACCCTCTCCACTGACAGAAAATTT
GTGCCATTAACATCACCATCTAATTCAACAAGAATTGGGACAACCTCCAG
TGAAAAGTTCTTCTCTTTACGCATCTAGTACTTTCTGTGTGACTCTAG
TATTTATTCGACTATAACAAACCATTTTCTTGCCTAAACCTGTACGATCC
TACAGGCTCTCTAGTATATAAACGCAAAAAGGGCCACCCCGAAGGGTGAGC
CAGTGTGACTCTAATAGAGAGCGGTCACCGACAAACAACAGAAAAAACG
AAAGGCCAGTCTTTTCGAACGGAACCTTTTTCGTTTTAATTTGAATGCCT
GGGTCTTAATATTTATTTAAAAAAGAAAAAGAAACCAAAATTTTACGG
GCCATAAGGGGGCCGCCCTCCCCCGCGGAAGAAAACCCCCCAAGAG
AAATTTTGGGTAAAAAACAATTTTAAAGTTTAAAGGGGGGGGAAAA
CACACCCCTCCTTGTGTCTCAAATAAGATATATAAAAAAGGGGGGGTT
TTTTTCGCCCGCAAAAAAATAAAAAA

Note:

Highlight (green, 69-944): E0240, GFP generator;

Highlight (yellow, 953-1007): R0062, pLux promoter;

GFP-C-Forward

Sequence: GGCATGGATGAACTATACAAATAA

Description: Forward, starting from the C terminal of GFP

Sequencing with GFP-C-Forward showed that the sequence was the same as expected – terminator (red), and pSB1A3 backbone (light grey) – which indicated a lack of mutation. Sequencing results are as follows:

> LasR-pLux-PF-GFPC-F 1334 ABI

1→

AGGAGCCAGGGCATCAATAAAACGAAAGGCTCAGTCGAAAGACTGGGCCT

TTCGTTTTATCTGTTGTTTGTTCGGTGAACGCTCTCTACTAGAGTCACACT
GGCTCACCTTCGGGTGGGCCTTTCTGCGTTTATA TACTAGTAGCGGCCGC
TGCAGGCTTCCTCGCTCACTGACTCGCTGCGCTCGGTCGTTTCGGCTGCGG
CGAGCGGTATCAGCTCACTCAAAGGCGGTAATACGGTTATCCACAGAATC
AGGGGATAACGCAGGAAAGAACATGTGAGCAAAGGCCAGCAAAGGCCA
GGAACCGTAAAAAGGCCGCGTTGCTGGCGTTTTTCCACAGGCTCCGCCCC
CCTGACGAGCATCACAAAATCGACGCTCAAGTCAGAGGTGGCGAAACCC
GACAGGACTATAAAGATAACCAGGCGTTTCCCCCTGGAAGCTCCCTCGTGC
GCTCTCCTGTTCCGACCCTGCCGCTTACCGGATACCTGTCCGCCTTTCTC
CCTTCGGGAAGCGTGGCGCTTTCTCATAGCTCACGCTGTAGGTATCTCAG
TTCGGTGTAGGTCGTTTCGCTCCAAGCTGGGCTGTGTGCACGAACCCCCG
TTCAGCCCGACCGCTGCGCCTTATCCGGTAACTATCGTCTTGAGTCCAAC
CCGGTAAGACACGACTTATCGCCACTGGCAGCAGCCACTGGTAACAGGAT
TAGCAGAGCGAGGTATGTAGGCGGTGCTACAGAGTTCTTGAAGTGGTGGC
CTAACTACGGCTACACTAGAAGAACAGTATTTGGTATCTGCGCTCTGCTG
AAGCCAGTTACCTTCGGA AAAAGAGTTGGTAGCTCTTGATCCGGCAAACA
AACCACCGCTGGTAGCGGTGGTTTTTTTTGTTTGCAAGCAGCAGATTACGC
GCAGAAAAAAAGGATCTCAAGAAGATCCTTTGATCTTTTCTACGGGGTCT
GACGCTCAGTGGAACGAAAACCTCACGTTAAGGGATTTTGGTCATGAGATT
ATCAAAAAGGATCTTACCTAGATCCTTTTAAATAAAAAATGAAGTTTTA
AATCAATCTAAAGTATATATGAAGTAAACTTGGTCTGACAGTTACCAATG
GCTTAATCAGTGAGGCACCTTATCTCAACGGATCTGTCTTATTTTCGTTCA
TCCCATAATTGGCCTGAACTCCCCCGTCCGTGGAAAAAAAACCTTACAAAA
CCGGGGGGGGGGCTTTACCCATTTCGGGGGGCCCCCAGGGGGGGTGCCAAG
GGAGAAAACCCCGCGCAAAAAACCCCCCGCCCCCCCCCGGGGGGCCTC
CCCAAAAAAATTTTTATTATTTAACACCCAAAA

Note:

Highlight (red, 6-134): B0015, Terminator;

Highlight (light grey, 151-1182): pSB1A3, vector backbone (part).

Supplemental References:

Bakshi, S., Siryaporn, A., Goulian, M., and Weisshaar, J.C. (2012). Superresolution imaging of ribosomes and RNA polymerase in live *Escherichia coli* cells. *Mol. Microbiol.* 85, 21 – 38.

Basu, S., Gerchman, Y., Collins, C.H., Arnold, F.H., and Weiss, R. (2005). A synthetic multicellular system for programmed pattern formation. *Nature* 434, 1130 – 1134.

Craig, N.L. (2002). *Mobile DNA II* (ASM Press).

Danino, T., Mondragón-Palomino, O., Tsimring, L., and Hasty, J. (2010). A synchronized quorum of genetic clocks. *Nature* 463, 326 – 330.

Ellis, T., Wang, X., and Collins, J.J. (2009). Diversity-based, model-guided construction of synthetic gene networks with predicted functions. *Nat. Biotechnol.* 27, 465 – 471.

Gillespie, D.T. (1977). Exact stochastic simulation of coupled chemical reactions. *J. Phys. Chem.* 81, 2340 – 2361.

Milo, R., Jorgensen, P., Moran, U., Weber, G., and Springer, M. (2010). BioNumbers--the database of key numbers in molecular and cell biology. *Nucleic Acids Res.* 38, D750 – 753.

Sayut, D.J., and Sun, L. (2010). Slow activator degradation reduces the robustness of a coupled feedback loop oscillator. *Mol. Biosyst.* 6, 1469 – 1474.

Sousa, A., Bourgard, C., Wahl, L.M., and Gordo, I. (2013). Rates of transposition in *Escherichia coli*. *Biol. Lett.* 9, 20130838.

Wu, M., Su, R.-Q., Li, X., Ellis, T., Lai, Y.-C., and Wang, X. (2013). Engineering of regulated stochastic cell fate determination. *Proc. Natl. Acad. Sci. U. S. A.* 110, 10610 – 10615.

Zhou, J.X., Aliyu, M.D.S., Aurell, E., and Huang, S. (2012). Quasi-potential landscape in complex multi-stable systems. *J. R. Soc. Interface R. Soc.* 9, 3539 – 3553.